

Published in final edited form as:

Nat Genet. 2015 December ; 47(12): 1408–1410. doi:10.1038/ng.3427.

Recurrent inactivating *RASA2* mutations in melanoma

Rand Arafah¹, Nouar Qutob¹, Rafi Emmanuel¹, Alona Keren-Paz¹, Jason Madore², Abdel Elkahoun³, James S. Wilmott², Jared J. Gartner⁴, Antonella Di Pizio⁵, Sabina Winograd-Katz¹, Sivasish Sindiri⁴, Ron Rotkopf⁶, Ken Dutton-Regester⁷, Peter Johansson⁷, Antonia Pritchard⁷, Nicola Waddell⁷, Victoria K. Hill³, Jimmy C. Lin⁴, Yael Hevroni¹, Steven A. Rosenberg⁴, Javed Khan⁴, Shifra Ben-Dor⁶, Masha Y. Niv⁵, Igor Ulitsky⁸, Graham J Mann^{2,9}, Richard A. Scolyer^{2,10,11}, Nicholas K. Hayward⁷, and Yardena Samuels^{1,*}

¹Molecular Cell Biology Department, Weizmann Institute of Science, Rehovot, Israel

²Melanoma Institute Australia and the University of Sydney, NSW, Australia

³National Human Genome Research Institute, National Institutes of Health, Bethesda, MD, 20892, USA

⁴National Cancer Institute, National Institutes of Health, MD, 20892, USA

⁵Institute of Biochemistry, Food Science and Nutrition, The Hebrew University, Rehovot, Israel

⁶Department of Biological Services, Weizmann Institute of Science, Rehovot, Israel

⁷QIMR, Berghofer Medical Research Institute, Brisbane, QLD, 4006, Australia

⁸Department of Biological Regulation, Weizmann Institute of Science, Rehovot, Israel

⁹Centre for Cancer Research, Westmead Millennium Institute for Medical Research, University of Sydney, NSW, Australia

¹⁰Discipline of Pathology, Sydney Medical School, The University of Sydney, Sydney, NSW, Australia

¹¹Tissue Pathology and Diagnostic Oncology, Royal Prince Alfred Hospital, NSW, Australia

Abstract

Users may view, print, copy, and download text and data-mine the content in such documents, for the purposes of academic research, subject always to the full Conditions of use: http://www.nature.com/authors/editorial_policies/license.html#terms

*To whom correspondence should be addressed: Yardena.Samuels@weizmann.ac.il.

URLs. Sequence data reported in this paper are available for download from dbSNP (http://www.ncbi.nlm.nih.gov/projects/SNP/snp_viewBatch.cgi?sbid=1062266)

All the statistical calculations were performed in the R statistical environment (<http://www.r-project.org>).

Accession Codes. *RASA2*, NM_006506, *BRAF* NM_004333, *NRAS* NM_002524, *NF1* NM_001042492

Author contributions

R.A., N.Q., R.E., A.K.P., J.J.G., and Y.S. designed the study J.M., A.E., J.S.W., J.J.G., K.D.R., P.J., A.P., N.W., G.J.M., R.A.S., N.K.H. and S.A.R. collected and analyzed the melanoma samples; S.S., R.R., J.C.L., J.K., S.B.D., I.U., analyzed the genetic data, R.A., R.E., S.W.K., V.K.H., Y.H and J.M. performed and analyzed the functional data. A.D.P. and M.Y.N performed the structure analysis. All authors contributed to the final version of the paper.

Competing Financial Interests

The authors declare no competing financial interests.

Analysis of 501 melanoma exomes revealed *RASA2*, encoding a RasGAP, as a tumor-suppressor gene mutated in 5% of melanomas. Recurrent loss-of-function mutations in *RASA2* were found to increase RAS activation, melanoma cell growth and migration. *RASA2* expression was lost in 30% of human melanomas and was associated with reduced patient survival. These findings reveal *RASA2* inactivation as a melanoma driver and highlight the importance of Ras GAPs in cancer.

Cutaneous melanoma, for which incidence rates continue to increase 1, represents a significant health problem worldwide. Recent genomic studies of melanoma 2,3,4 have discovered several driver genes and enabled development of targeted drugs, which show promise in treating melanoma patients 5,6. However, responses are rarely durable; therefore there is an urgent need to identify additional targetable alterations in melanoma.

Most approved drugs that target genetically altered proteins in cancer are towards kinases 7. However, a majority of the proteins mutated in cancer are tumor suppressors which cannot be re-activated by small molecules. A possible solution is exploiting the fact that tumor suppressor gene inactivation results in activation of a downstream growth pathway. For example, *PTEN* mutations lead to increased activity of the downstream kinase *AKT* 8. In this study we sought to systematically identify tumor suppressor genes in melanoma and characterize the downstream pathways activated by their loss of function.

We compiled somatic mutation data from whole exome/genome sequence of 501 melanomas from various sources including The Cancer Genome Atlas (TCGA) 2,3. Data were analyzed as described previously 9 (Supplementary Table 1 and 2). Genes were ranked based on non-synonymous mutation frequency, number of mutations per megabase and mutation burden 9. We then identified genes for which nonsense or frameshift mutations encompass at least 20% of all its mutations, a suggested threshold for tumor suppressor genes 10. The highest ranking genes were *TP53*, *NFI*, *ARID2*, *CDKN2A*, and *PTEN*. After these, we found *RASA2* was mutated in 5.4% of patients (Table 1) and 27% of those mutations were alterations leading to loss of function (LOF) (Table 1). The distribution of the 32 non-synonymous mutations identified in *RASA2* is shown in Fig. 1A. We profiled the copy number landscape of 22 samples using the CytoScan High Definition array (Affymetrix) and found 3 focal deletions (13.6%). Consistent with these data, examination of the melanoma TCGA copy number variation (CNV) data, showed deletions of the *RASA2* locus in 11.7% of cases. Furthermore, *RASA2* was found to be null in 1% of melanoma samples investigated, placing *RASA2* in the top 10% of all homozygously deleted genes in the TCGA data ($p < 0.05$). Thus, *RASA2* is a potential tumor suppressor gene in melanoma (Table 1, Supplementary Table 2 and Supplementary Fig. 1).

RASA2 encodes a GTPase-activating protein (GAP), which stimulates the GTPase activity of wild-type (WT) RAS but not its mutated oncogenic form. Acting as a suppressor of RAS function, *RASA2* enhances the weak intrinsic GTPase activity of RAS resulting in the inactive GDP-bound isoform 11. Importantly the role of *RASA2* has never been investigated in melanoma. Recently, *NFI*, which encodes another RAS-specific GAP, has been found frequently mutated and to play a central role in melanoma 2,3. Mutations in *RASA2* and *NFI* co-occur strongly (p -value: 0.000011 [Fisher's Exact Test] (Fig. 1B; Supplementary

Table 3). Examination of publicly available databases revealed that *RASA2* is mutated in several other tumor types (Supplementary Fig. 2).

To test whether *RASA2* is a tumor suppressor in melanoma, we knocked down its expression in immortalized, non-tumorigenic NIH3T3 cells, using two short hairpin RNA (shRNA) constructs. *RASA2* knockdown resulted in RAS activation (Supplementary Fig. 3A), leading to increased cell growth on plastic and in soft agar (Supplementary Fig. 3B).

To characterize the tumorigenic effects of *RASA2* in melanoma cells, we functionally characterized two recurrent *RASA2* mutations: p.Arg310*, which causes *RASA2* truncation, and p.Ser400Phe in the catalytic RAS-GAP domain. We established stable pooled clones expressing vector control, WT or mutant *RASA2* in the melanoma cell lines A375 (BRAF V600E, NRAS WT, NF1 mutant), 501Mel (BRAF V600E, NRAS WT, NF1 WT), 108T (BRAF WT, NRAS WT, NF1 mutant) and 55T (BRAF WT, NRAS WT, NF1 mutant) which all express WT *RASA2*. We detected similar levels of overexpressed *RASA2* protein in A375, 501Mel, 108T and 55T stable clone cell lines except for the p.Arg310* mutant in 108T, which had increased protein expression (Supplementary Fig. 4). These clones were used for subsequent studies.

Since *RASA2* encodes a RAS GAP, we hypothesized that *RASA2* mutation or loss would alleviate RAS suppression. Indeed, modeling the *RASA2* mutants on the structure of p120GAP 12 predicts that the *RASA2* p.Arg310* mutant is unable to bind to Ras as it lacks the RAS-GAP, PH and BTK domains. Although the *RASA2* p.Ser400Phe mutant is expected to bind Ras, the mutation is likely to affect the stabilization of its catalytic site, which may disturb structural changes necessary for GAP catalysis, leading to increased Ras activity (Supplementary Fig. 5). To test the effects of *RASA2* on RAS, we conducted both gain and loss-of-function studies. Overexpression of WT *RASA2* substantially suppressed RAS-GTP levels; in contrast, both *RASA2* mutants failed to suppress RAS-GTP levels, demonstrating that these two mutations result in a clear loss of function (Fig. 1C and Supplementary Fig. 6A). The mutations were not found to have this effect in A375 cells due to their high BRAF activity. This is consistent with previous data indicating that above a certain threshold of active protein, RAS can lead to maximal pathway activation 13. The A375 clones were therefore not analyzed further in this study. Conversely, in melanoma cells that retained *RASA2* expression, RNA interference (RNAi)-mediated suppression of *RASA2* led to the activation of RAS in 501Mel and 108T (Fig. 1C middle, 1C right). Endogenous *RASA2* in 55T was barely detectable by immunoblotting (Supplementary Fig. 4B), for this reason, *RASA2* knockdown in this cell line was not performed. Importantly, re-introduction of WT *RASA2* into melanoma cells that harbor *RASA2* mutations (76T: p.Arg310* and C084: p.Ser400Phe) inhibited RAS activation (Supplementary Fig. 6B). These data confirm that *RASA2* is a functional RAS GAP and that mutation or loss of *RASA2* activates RAS in melanoma. The variation seen in the effects of *RASA2* mutants on RAS-GTP levels are probably due to differences in the cells lines' mutational background and variation in endogenous *RASA2* protein abundance as these can modulate RAS-complex formation and are important in context-dependent signaling, as shown by Kiel *et al* 14. Furthermore, in some cases, the *RASA2* mutants were found to enhance RAS-GTP

levels, suggesting that these variants may have dominant negative effects. This scenario has precedent and has been described for p53 and PTEN 15,16.

To examine the effects of *RASA2* mutations on proliferation and colony forming ability, we investigated cell growth *in vitro*. In low serum-containing media, WT clones grew slower than mutant clones (Fig. 1D and Supplementary Fig. 7A). We also observed this difference in anchorage independent cell growth, where cells expressing mutant *RASA2* formed a significantly higher number of colonies compared to WT *RASA2* (Fig. 1E and Supplementary Fig. 7Ci; $P < 0.005$ *t*-test). In agreement with the tumor suppressor role of *RASA2*, overexpression of WT *RASA2* in melanoma cells that harbor *RASA2* mutations (C084 and 76T) led to reduced cell growth (Supplementary Fig. 7B) and diminished anchorage independent growth (Supplementary Fig. 7Cii).

As previous studies reported that activation of RAS increases cell migration 17, we examined whether mutated *RASA2* had the same effect. After seeding 108T, 55T or 501Mel pooled clones in serum-free medium, WT *RASA2* expression led to reduced cell migration, whereas mutant *RASA2* expression failed to suppress migration (Supplementary Fig. 8; $P < 0.0001$ *t*-test).

To validate the extent to which *RASA2* protein expression is lost in human melanomas and to assess its prognostic potential, we performed *RASA2* immunohistochemistry (IHC) on a set of AJCC stage III melanomas (Supplementary Fig. 9) 18 19 . We found that *RASA2* expression was negative in 33% (27 of 81) of cases and positive in 67% (54 of 81) of melanomas (Supplementary Fig. 9C). Kaplan-Meier plot and log-rank tests showed that loss of *RASA2* expression (negative by IHC) was significantly associated with poorer survival, HR=0.42 (0.23-0.78), Log rank $p=0.0043$ (Fig. 1F). These results further emphasize the role of *RASA2* loss in melanoma progression and indicate it has prognostic relevance.

The finding of common alterations in *RASA2*, together with functional data indicating its effect on cell growth and migration, suggest that *RASA2* is an important tumor suppressor in human melanoma. Particularly important is the fact that *RASA2* suppression provides an alternative mechanism of RAS activation. This study demonstrates that melanomas have somatic mutations in the *RASA2* gene, which lead to impaired *RASA2* activity and constitutive activation of RAS signaling.

Materials and Methods

Tumor tissues

All DNA samples used in this study were derived from metastases. Samples used for whole-exome capture were extracted from cell lines established directly from patient tumors as described previously 20. DNA subjected to whole-genome sequencing was extracted from OCT embedded specimens as described previously 20. Tissue was further collected and cell lines established at QIMR Berghofer Medical Research Institute. All cell lines were established as described previously 21 with informed patient consent under a protocol approved by the QIMR Berghofer Medical Research Institute Human Research Ethics Committee.

A subset of cell lines used in the study (108T, 55T and 76T) were derived from a panel of pathology-confirmed metastatic melanoma tumor resections collected from patients enrolled in IRB-approved clinical trials at the Surgery Branch of the National Cancer Institute. Pathology-confirmed melanoma cell lines were derived from mechanically or enzymatically dispersed tumor cells, which were then cultured in RPMI 1640 + 10% FBS at 37°C in 5% CO₂ for 5-15 passages. The C084 cell line was established at QIMR Berghofer Medical Research Institute as described previously 21, with informed patient consent under a protocol approved by the QIMR Berghofer Medical Research Institute Human Research Ethics Committee. Cell lines genotypes are indicated in Supplementary Table 6. All cell lines have been tested negative for mycoplasma.

PCR, sequencing and mutational analysis

PCR and sequencing of *RASA2* was done as previously described 22. Sequence traces were analyzed using the Mutation Surveyor software package (SoftGenetics). Primers used are listed in Supplementary Table 4. Data deposition: The sequence reported in this paper will be deposited in the dbSNP, ClinVar database.

Statistical analyses

To evaluate whether the frequency of somatic mutations is significantly higher than would be expected if the mutations were neutral, we performed the following statistical test. The null hypothesis was that the probability of a mutation at a specific base is the neutral rate of 11.4 mutations/Mb (i.e. $p=11.4 \times 10^{-6}$). We computed a one-sided p-value using the `pbinom` function in the R statistical software. To determine whether the ratio of nonsynonymous to synonymous mutations observed was statistically significant, the exact binomial test was used, with an expected ratio of 2.5:1.9. Sample size considered a binomial distribution based on the number of base pairs sequenced for the gene of interest, the number of mutations observed and the background rate of mutation. For the background rate, we used the observed rate in the exome screen: 11.2 mutations per Mb. With this study design, there is more than 99% probability of identifying a gene that is mutated at 1% or higher. All the statistical calculations were performed in the R statistical environment. Further statistical analyses were performed using Microsoft Excel to generate p-values to determine significance (two-tailed t-test). Red arrows in Figure 1 include frameshift, nonsense and deleterious mutations based on SIFT analysis.

CytoScan array processing and analysis

Samples were prepared according to Affymetrix protocols (Affymetrix, Inc). DNA quality and quantity was ensured using Bioanalyzer (Agilent, Inc) and NanoDrop (Thermo Scientific, Inc) respectively. Per DNA labeling, 200 nanograms of genomic DNA were used in conjunction with the Affymetrix recommended protocol for CytoScan HD array kit and reagents (catalog# 901835). The hybridization cocktail containing the fragmented and labeled DNAs was hybridized to The Affymetrix CytoScan HD GeneChip. The chips were washed and stained by the Affymetrix Fluidics Station using the standard format and protocols as described by Affymetrix. The probe arrays were stained with streptavidin phycoerythrin solution (Molecular Probes, Carlsbad, CA) and enhanced by using an antibody solution containing 0.5 mg/mL of biotinylated anti-streptavidin (Vector

Laboratories, Burlingame, CA). An Affymetrix Gene Chip Scanner 3000 was used to scan the probe arrays. The .Cel files were generated from the scanned images using Affymetrix AGCC software and the .cyhd.cychp files were generated by the Chromosome Analysis Suite (ChAS) Version 2.1 software.

All the analyses were done with ChAS default parameters for LOH and Copy Number State (CNS). A description of the samples used for this analysis is listed in Supplementary Table 5.

Construction of wild-type and mutant *RASA2* expression vectors

Human *RASA2* cDNA (NM_006506) was cloned from HEK293T cDNA using PfuUltra II Hotstart PCR Master Mix (Agilent Technologies, Santa Clara, CA) according to manufacturers' instructions and the forward and reverse primers in Supplementary Table 8. A FLAG tag was introduced onto the N-terminus of *RASA2* during the cloning procedure. PCR products were cloned into the pCDF1-MCS2-EF1-Puro vector (Systems Biosciences, Inc., Mountain View, CA) via the XbaI and NotI restriction sites. The p.S400F mutation was introduced using fusion PCR site directed mutagenesis. The p.R310X mutation was created by using an alternative reverse primer to introduce the relevant nonsense mutation/stop codon.

Western blotting

501Mel, 108T and 55T cells stables with *RASA2*-FLAG (WT, mutant or empty vector) were gently washed 2X in PBS and then lysed using 1.0 ml 1% NP-40 lysis buffer (1% NP-40, 50 mM Tris-HCl pH 7.5, 150 mM NaCl, Complete Protease Inhibitor tablet, EDTA-free (Roche, Indianapolis, IN), 1 μ M sodium orthovanadate, 1 mM sodium fluoride, and 0.1% β -mercaptoethanol) per T-75 flask for 20 minutes on ice. Lysed cells were scraped and transferred into a 1.5 mL microcentrifuge tube. Extracts were centrifuged for 10 minutes at 14,000 rpm at 4°C. Proteins (50 μ g) were resolved on 10% SDS-polyacrylamide gels and transferred to nitrocellulose membranes (BioRad). Western blots were probed with the following antibodies anti-FLAG (M2) (Sigma-Aldrich) and GAPDH (Millipore). Ras-GTP levels were determined using a RAS activation Assay Kit (EMD Millipore). Every Ras-GTP assay was performed twice.

Pooled stable expression

To produce lentivirus, *RASA2* constructs were co-transfected into HEK 293T cells seeded at 2.5×10^6 per T75 flask with pVSV-G and pFIV-34N (kind gifts from Todd Waldman, Georgetown University) helper plasmids using Lipofectamine 2000 (Life Technologies) as described by the manufacturer. Virus-containing media was harvested 60 hr after transfection, filtered, aliquoted and stored at -80°C.

501Mel, 55T and 108T cells were grown in RPMI-1640 (Biological Industries) and supplemented with 10% fetal bovine serum (HyClone, Logan, UT). Lentivirus for *RASA2* (WT, p.Arg310* and S400F) and empty vector control were used to infect the cells as previously described 23. Stable expression of *RASA2* proteins (WT and mutants) was

determined by SDS-PAGE analysis followed by immunoblotting with anti-FLAG and anti-GAPDH to show equivalent expression among pools.

siRNA depletion of endogenous RASA2

Two human RASA2 specific siRNAs (ON-Targetplus) were designed using siRNA design program for human *RASA2* and were purchased from Dharmacon (Thermo Fisher Scientific). The sequences of the two siRNAs used to transiently deplete *RASA2* in malignant melanoma cells are found in Supplementary Table 7. Using DharmaFECT transfection reagent #1 (specific for siRNA), melanoma cells were transfected with 50 nM siRNA On target siRNA in the presence of OptiMEM-I medium (Life Technologies). Cells were incubated for 72 h post-transfection before checking RAS-GTP levels by the RAS Activation Assay Kit (Millipore).

Lentiviral shRNA

All shRNA expression constructs were obtained from Open Biosystems. Lentiviral stocks were prepared as previously described²². NIH 3T3 cells were infected with shRNA for each condition (vector control and two independent mouse *RASA2*-specific shRNAs) and selected as previously described²². The shRNA constructs used in this study were: sh50 (TRCN0000034350) and sh51 (TRCN0000034351).

3D Ras-RASA2 model prediction

The complex between human HRAS bound to guanosine triphosphatase (GTPase)-activating domain of the human GTPase-activating protein p120GAP (GAP-334), 1WQ1.pdb²⁴, was used as a template to create both RASA2 (1WQ1 chain G, GAP-334) and Mg²⁺-NRAS-GTP (1WQ1 chain R, HRAS) models. GAP-334 sequence present in the PDB file is shorter than RASA2, but it covers the binding interface, is bound to RAS, and has high similarity with the query. Sequence alignment and homology modeling were performed with Prime (version 4.0, Schrödinger, LLC, New York, NY, 2014). The initial X-ray structure 1WQ1 contains the substrate GDP-AIF3 bound to HRAS. AIF3 molecule, that is thought to mimic the γ -phosphate moiety of GTP²⁴, was manually replaced with the γ -phosphate group bound to GDP.

Hydrogen atoms and side chain orientations of the GTP-NRAS-RASA2 complex were optimized with the Protein Preparation Wizard tool from Schrödinger at physiological pH. Side chains were refined with the Predict Side Chains tool available in Prime. Both complexes GTP-NRAS-(WT)RASA2 and GTP-NRAS-(S400F)RASA2 were then minimized to a derivative convergence of 0.05 kJ/mol-Å using the Polak-Ribiere Conjugate Gradient (PRCG) minimization algorithm, the OPLS2005 force field and the GB/SA water solvation model implemented in MacroModel (version 10.8, Schrödinger, LLC, New York, NY, 2014): the finger loop was set to be free to move, a shell 5 Å around the loop minimized applying a force constant of 200 kJ/molÅ², and another shell of 5 Å with a constant force of 300 kJ/molÅ².

Proliferation assays

To examine cell growth, melanoma cell lines (501Mel, 55T and 108T) stably infected with either vector, WT RASA2, p.Arg310* mutant or p.Ser400Phe mutant RASA2 were seeded in 6 replicates into 96 well plates at 200-2000 cells per well and incubated for 7-17 days. Samples were analyzed every 48 hrs by lysing cells in 50 μ l 0.2% SDS/well and incubating for 2 hour at 37°C prior to addition of 150 μ l/well of SYBR Green I solution (1:750 SYBR Green I (Invitrogen-Molecular Probes) diluted in dH₂O).

Soft agar assay

501Mel, 108T and 55T pooled RASA2 clones were plated in 4 replicates at 1000 cells/well in top plugs consisting of sterile 0.33% Bacto-Agar (BD, Sparks, MD) and 2.5% fetal bovine serum (HyClone, Logan, UT) in a 24-well plate. The lower plug contained sterile 0.5% Bacto-Agar and 2.5% fetal bovine serum. After one week, the colonies were counted.

Migration Assay

Blind well chemotaxis chambers with 13-mm diameter, 8mm pore size PVPF filters (Costar Scientific Co, Cambridge, MA) were used. Cells (2×10^5) suspended in serum free medium, were added to the upper chamber. 10% FBS full medium was placed in the lower chamber. Assays were carried out at 37 degrees in 5% CO₂. After incubation (12-24h), the upper surface of the filter was freed of the cells by using a cotton swab. Cells that passed through the filter to the bottom side were fixed in methanol and then stained by Geimsa. Each triplicate assay was performed three times. Migrating cells were counted blindly in ten representative light-microscopy fields.

RASA2 immunohistochemistry

RASA2 immunohistochemistry (IHC) was performed on AJCC Stage III melanoma tumor microarrays (TMAs). It was performed using rabbit polyclonal anti-RASA2 antibody from Sigma-Aldrich (HPA035375) on a DAKO IHC autostainer using DAKO EnVison FLEX+ detection system (DAKO; K8002) with DAB as the chromogen (DAKO; K3467) as per the manufacturers' instructions (high pH antigen retrieval, primary antibody dilution 1:100 for 60 min). Resultant predominant IHC signal was cytoplasmic. Cases were scored as a percent of cytoplasmic positive tumor cells (0-100) and overall tumor staining intensity (0 - 4). Typically in positive samples, there was homogeneous staining across 100% of tumor cells. The intensity of staining varied between patients and ranged from negative (intensity = 0) to weakly positive (intensity 1 - 2) or strongly positive (intensity 3 - 4). Cases were scored as percent of cytoplasmic positive tumor cells (0-100) and overall tumor staining intensity (0 - 4). The Kaplan Meier graph represents negative (intensity = 0) versus any positive (1-4).

TMA cohort description

Samples eligible for this TMA were obtained at the Melanoma Institute Australia Biospecimen Bank from AJCC stage-III (lymph node) metastatic melanoma specimens in which macroscopic tumor was observed, from patients believed to be without distant metastases at the time of tumor banking based on clinical examination and computerized axial tomographic scanning of the brain, chest, abdomen, and pelvis. Key covariates were

balanced in this cohort to permit survival analysis. These samples were used to derive Figure 1F

Supplementary Material

Refer to Web version on PubMed Central for supplementary material.

Acknowledgements

We thank T. Wiesel for graphical assistance. This work was supported by the Intramural Research Programs of the National Human Genome Research Institute and National Cancer Institute, as well as program grants of the Australian National Health and Medical Research Council (NHMRC) and the Cancer Institute NSW. YS is supported by the Israel Science Foundation grant numbers 1604/13 and 877/13, the European Research Council (ERC) (StG-335377), the European Research Council (ERC) under the European Union's Horizon 2020 research and innovation program (grant agreement No 677645)", by the Henry Chanoch Kreter Institute for Biomedical Imaging and Genomics, the estate of Alice Schwarz-Gardos, the estate of John Hunter, the Knell Family, the Peter and Patricia Gruber Award and the Hamburger Family. IU is supported by a grant from The Rising Tide Foundation. NKH, KD-R and RAS are supported by fellowships from the NHMRC. ALP is supported by Cure Cancer Australia. Support from Melanoma institute Australia is also gratefully acknowledged. We thank the TCGA Research Network for generating some of the datasets.

References

1. Siegel R, Naishadham D, Jemal A. *CA Cancer J Clin.* 2012; 62:283–98. [PubMed: 22987332]
2. Hodis E, et al. *Cell.* 2012; 150:251–63. [PubMed: 22817889]
3. Krauthammer M, et al. *Nat Genet.* 2012; 44:1006–14. [PubMed: 22842228]
4. Krauthammer M, et al. *Nat Genet.* 2015; 47:996–1002. [PubMed: 26214590]
5. Flaherty KT, et al. *N Engl J Med.* 2010; 363:809–19. [PubMed: 20818844]
6. Chapman PB, et al. *N Engl J Med.* 2011; 364:2507–16. [PubMed: 21639808]
7. Lemmon MA, Schlessinger J. *Cell.* 2010; 141:1117–34. [PubMed: 20602996]
8. Vivanco I, Sawyers CL. *Nat Rev Cancer.* 2002; 2:489–501. [PubMed: 12094235]
9. Sjoblom T, et al. *Science.* 2006; 314:268–74. [PubMed: 16959974]
10. Vogelstein B, et al. *Science.* 2013; 339:1546–58. [PubMed: 23539594]
11. Maertens O, Cichowski K. *Adv Biol Regul.* 2014; 55:1–14. [PubMed: 24814062]
12. Miao W, Eichelberger L, Baker L, Marshall MS. *J Biol Chem.* 1996; 271:15322–9. [PubMed: 8663024]
13. Rodriguez-Viciano P, Oses-Prieto J, Burlingame A, Fried M, McCormick F. *Mol Cell.* 2006; 22:217–30. [PubMed: 16630891]
14. Kiel C, Verschuere E, Yang JS, Serrano L. *Sci Signal.* 2013; 6:ra109. [PubMed: 24345680]
15. Ko LJ, Prives C. *Genes Dev.* 1996; 10:1054–72. [PubMed: 8654922]
16. Papa A, et al. *Cell.* 2014; 157:595–610. [PubMed: 24766807]
17. Fang JY, Richardson BC. *Lancet Oncol.* 2005; 6:322–7. [PubMed: 15863380]
18. Mann GJ, et al. *J Invest Dermatol.* 2013; 133:509–17. [PubMed: 22931913]
19. Jayawardana K, et al. *Int J Cancer.* 2015; 136:863–74. [PubMed: 24975271]
20. Wei X, et al. *Nat Genet.* 2011; 43:442–6. [PubMed: 21499247]
21. Dutton-Regester K, et al. *Oncotarget.* 2014; 5:2912–7. [PubMed: 24913145]
22. Palavalli LH, et al. *Nat Genet.* 2009; 41:518–20. [PubMed: 19330028]
23. Solomon DA, et al. *Cancer Res.* 2008; 68:10300–6. [PubMed: 19074898]
24. Scheffzek K, et al. *Science (New York, N Y).* 1997; 277:333–8.

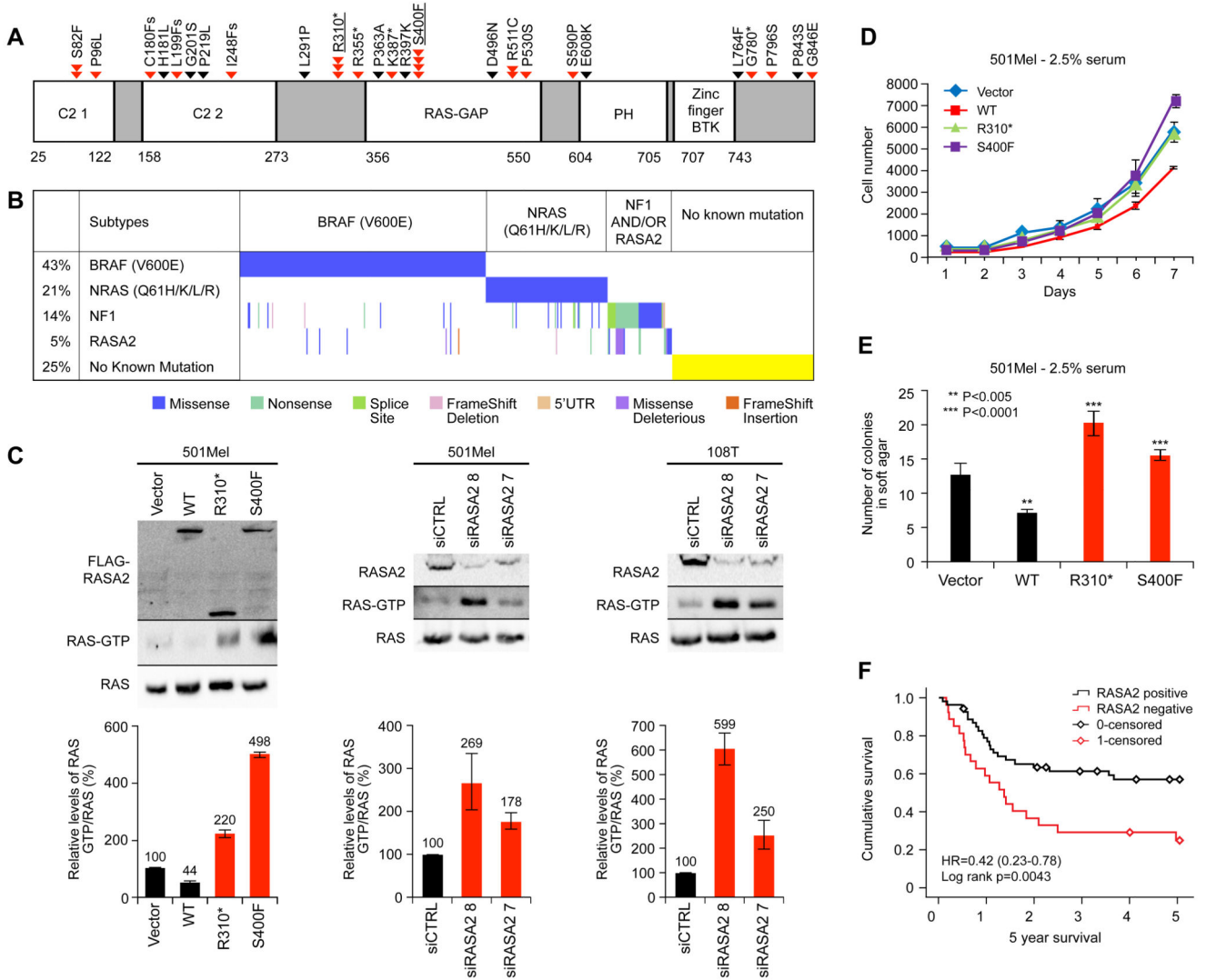


Figure 1. Effects of RASA2 mutations on RAS activity, growth and patient survival. (A) Human RASA2 protein, conserved domains indicated as blocks: C2 domain first repeat (C2 1); C2 domain second repeat (C2 2); Ras-GTPase activating domain (RAS-GAP); Plekstrin homology domain (PH); Bruton’s tyrosine kinase Cys-rich motif (BTK). Somatic mutations indicated with arrows and amino-acid changes. Red triangles indicate deleterious mutations. Underlined mutations were functionally assessed. (B) Distribution of somatic mutations in *BRAF*, *NRAS*, *NF1* and *RASA2* in melanoma (n=501). (C) Immunoblot of RAS-GTP levels in 501Mel cells expressing the indicated constructs (left). 501Mel cells (middle) and 108T (right) cells depleted for RASA2 using human *RASA2* siRNAs. RAS-GTP levels were assessed by RAS pull-down assay and the RAS-GTP/RAS ratio of 2 independent experiments were calculated and normalized to the vector control (lower panel). Error bars, standard deviation (S.D.) (D) 501Mel clones expressing the indicated constructs were seeded in 96-well plates in 2.5% FBS and average cell number was measured by assessing DNA content using SYBR Green I from two independent experiments with six repeats each. Error bars, standard deviation (S.D.).(E) Anchorage-independent proliferation

of 501Mel RASA2 clones expressing the indicated constructs was assessed by measuring colony formation in soft agar in 2.5% serum from two independent experiments four repeats each after 7 days. ** $P < 0.005$ for WT vs. vector and *** $P < 0.0001$ for WT vs mutants (Students t -tests). (F) Kaplan-Meier curve showing overall survival of AJCC stage III melanoma patients with positive (n=54) or negative (n=27) RASA2 expression (log rank $p = 0.0043$).

Table 1
Melanoma driver genes that harbor at least 20% loss of function mutations

Gene name	% of tumors with mutation	% LOF of all coding mutations
<i>TP53</i>	17.1	33.3
<i>NF1</i>	14.4	42.0
<i>ARID2</i>	12.6	53.0
<i>CDKN2A</i>	12.4	57.6
<i>PTEN</i>	8.8	44.4
<i>SETD2</i>	5.4	32.4
<i>RASA2</i>	5.4	27.3

Genes were ranked based on the non-synonymous frequency, mutations per megabase, mutation rate (taking into account the base coverage) and presence of deleterious (nonsense or frameshift) mutations in at least 20% of the cases.